Asian Journal of Chemistry; *Vol. 32, No. 12 (2020), 3057-3062*

ASIAN JOURNAL OF CHEMISTRY

https://doi.org/10.14233/ajchem.2020.22945

NMR & Electronic Spectra, NLO, FMO, NBO and Thermodynamic Properties of Pentachlorophenol: An Experimental and Theoretical Investigation

P. VENKATA RAMANA RAO[1,*], K. SRISHAILAM[1], G. RAMESH[2], B. VENKATRAM REDDY[3,*] and G. RAMANA RAO[3]

[1]Department of Physics, SR University, Warangal-506371, India
[2]Department of Physics, University P.G. College (Satavahana University), Godavarikhani-505208, India
[3]Department of Physics, Kakatiya University, Warangal-506009, India

*Corresponding authors: E-mail: poladi.ramana@gmail.com; bvreddy67@yahoo.com

Received: 14 August 2020; *Accepted*: 12 September 2020; *Published online*: 7 December 2020; AJC-20139

Proton (^1H) and Carbon-13 (^{13}C) nuclear magnetic resonance spectra of pentachlorophenol were measured. Corresponding chemical shifts were generated using Gauge Independent Atomic Orbital (GIAO) approach, as a part of density functional theory (DFT) application. UV-visible spectrum was measured in the spectral range 200-400 nm and compared with its simulated counterpart generated, using time-dependent density functional theory (TD-DFT). Frontier molecular orbital (FMO) approach was used to understand origin of UV-visible spectrum and chemical reactivity of the molecule. The non-linear (NLO) behaviour was studied by evaluating the values of dipole moment, polarizability and hyperpolarizability. Molecular electrostatic potential (MESP) surface was drawn to locate reactive sites of pentachlorophenol. Natural bond orbital (NBO) analysis of the molecule was made to examine stability of the molecule arising from charge delocalization. Thermodynamic parameters of the molecule were also calculated.

Keywords: Pentachlorophenol, DFT, Gauge independent atomic orbital, Chemical reactivity, FMO, NLO, NBO.

INTRODUCTION

Pentachlorophenol is a chlorinated aromatic compound, widely used as a biocide and could also be found in ropes, paints, adhesives, canvas, insulating materials and brick walls [1]. Pentachlorophenol is produced *via* two pathways, either by stepwise chlorination of phenols in the presence of catalysts (Lewis acid) or alkaline hydrolysis of hexachlorobenzene [1]. Toxicities of this biocide compound showed that pentachlorophenol is rapidly and efficiently absorbed from the gastrointestinal and respiratory tracts [2]. Once absorbed, pentachlorophenol exhibits a small volume of distribution. Metabolism occurs primarily in the liver, to a limited extent, *via* oxidative dechlorination and conjugation.

Pentachlorophenol can be metabolized by several aquatic and soil microorganisms, but environmental conditions are usually unfavourable for biodegradation [3-5]. Slow elimination in surface waters, high persistence in sediments, formation of stable metabolites and the limited adaptation of microorganisms to chlorophenols owing to their high microbial toxicity imply that chlorophenols are practically non-biodegradable in the aquatic environment [6].

By adopting classical inverse vibrational problem approach, the investigations regarding vibrational spectra, normal coordinate analysis and transferability of force constants of some substituted phenols were already reported in our earlier work [7,8]. At present, we are engaged with addressing problems associated with structure, vibrational properties, electronic characteristics, frontier molecular orbital (FMO) utility, non-linear optical (NLO) behaviour, natural bond orbital (NBO) analysis and thermodynamic parameters using both experimental (X-ray, ^1H NMR, ^{13}C NMR, FT-IR, FT-Raman, UV-vis) and theoretical (density functional theory *i.e.* DFT) tools [9,10], in addition to anticancer activity. Recently, the structural and vibrational properties for pentachlorophenol [11] and pentabromophenol [12] are reported. However, results of ^1H & ^{13}C NMR, UV-Vis spectrum, FMO, NLO, NBO and thermodynamic analysis for pentachlorophenol are yet to be reported. In present work, the results of ^1H & ^{13}C NMR, NLO properties, UV-visible spectrum (both experimental and simulated), frontier molecular orbitals (FMOs), molecular electrostatic potential (MESP) surface, chemical reactivity, natural bond orbital (NBO) analysis, thermodynamic parameters of pentachlorophenol are discussed.

EXPERIMENTAL

Sample of solid pentachlorophenol, in pure form, was obtained from Tokyo Kasei Kogyo Co. Ltd; Japan. It was used without further purification for spectral measurements. ^{1}H & ^{13}C NMR spectra of the sample were recorded by dissolving it in DMSO-d_6 at room temperature on Bruker Ascend-400 NMR spectrometer (^{13}C resonates at 100 MHz) and TMS was used as internal standard. UV-visible spectrum of pentachlorophenol was measured in the spectral range 200-400 nm at room temperature using Perkin-Elmer UV-Visible Lambda-25 double beam spectrometer employing 1 cm quartz cell. Dimethylformamide was used as a solvent.

Computational details: Required calculations were made by using Gaussian 09/DFT PROGRAM package [13]. Becke's three parameter hybrid exchange functional B3 [14], in combination with Lee-Yang-Parr (LYP) correlational functional [15], together with split valence triple basis set *i.e.*, 6-311++G(d,p) was used.

Chemical shifts in ^{1}H & ^{13}C NMR spectra were calculated employing Gauge Independent Atomic Orbital (GIAO) approach [16] with B3LYP/6-311++G(d,p) method with reference to TMS. Solvent effects were taken into account by the polarizable continuum model (PCM) using the integral equation formalism (IEF-PCM) variant [17] implemented in Gaussian 09 program package. The PCM method available in Gaussian 09 includes an external iteration procedure in order to compute the energy in solution by making the solvent reaction field self-consistent with the solute electrostatic potential obtained from the computed electron density with the specified model chemistry [18,19]. The program builds up van der Waals surface cavity using the universal force field (UFF) atomic radii, which places a sphere around each solute atom with the radii scaled by a factor of 1.1 and skips the generation of "added spheres" to smooth the surface. Resulting spectra were compared with corresponding experimental NMR spectra. Total molecular dipole moment (μ_t) and its components; total molecular polarizability (α_t) and its components; anisotropy of polarizability ($\Delta\alpha$) and first order static hyperpolarizability (β_t) were evaluated using density functional theory based on finite field approach, using Buckingham's definitions [20]. A rigid-rotator harmonic approximation was assumed. The analysis uses expressions for an ideal gas in the canonical ensemble [21]. The electronic absorption spectrum involving electronic transitions was calculated by means of time-dependent density functional theory (TD-DFT), with 6-311++G(d,p) basis set. Molecular electronic properties such as ionization potential (I), electron affinity (A), global hardness (η), chemical potential (μ) and global electrophilicity power (ω) of pentachlorophenol were obtained from frontier molecular orbital (FMO) energies comprising of HOMO (highest occupied molecular orbital) and LUMO (lowest unoccupied molecular orbital) using the following expressions [22-25].

$$I = -E_{HOMO}$$
$$A = -E_{LUMO}$$
$$\eta = (-E_{HOMO} + E_{LUMO})/2$$
$$\mu = (E_{HOMO}+E_{LUMO})/2; \text{ and}$$
$$\omega = \mu^2/2\eta$$

where E_{HOMO} and E_{LUMO} are HOMO and LUMO orbital energies. The energy of interaction of a positive point charge at position $\vec{r}$ with the nuclei and electrons of a molecule is known as the molecular electrostatic potential (MESP). It was obtained by using expressions available in literature [26,27]. To get an idea of various second order interactions between the filled orbitals of one subsystem and vacant orbitals of another subsystem, natural bond orbital (NBO) calculations were made, employing NBO 3.1 program [28] as implemented in the Gaussian 09W program package at the DFT/B3LYP level using 6-311++G(d,p) basis set. Such calculations are needed to quantify hyper conjugation (or delocalization). This is achieved by evaluating donor-acceptor interactions using second order perturbation theory analysis of Fock matrix in NBO basis of pentachlorophenol. The interactions manifest as loss of occupancy from the localized NBO of the idealized Lewis structure into an empty non-Lewis orbital. The stabilization energy associated with the delocalization is obtained from equation provided by Reed *et al.* [28] and Chocholousova *et al.* [29]. The thermodynamic parameters were also computed for pentachlorophenol by DFT method with B3LYP/6-311++G(d,p) basis set.

RESULTS AND DISCUSSION

Assignment of NMR chemical shifts: Experimental ^{1}H & ^{13}C NMR spectra of the sample and their simulated counterparts are displayed in Figs. 1 and 2. Experimental and theoretical chemical shifts of pentachlorophenol are presented in Table-1. The lone ^{1}H NMR signal calculated at 6.6 ppm was identified with experimental signal near 7.2 ppm and assigned to the proton of hydroxyl moiety (Fig. 1). The aromatic carbon in ^{13}C NMR spectra, in general, provides NMR signals in the δ_C (carbon chemical shift) range 110-135 ppm. Due to delocalization of π-charge of aromatic ring [9] and lone pair electrons of oxygen atom, the C1 atom acquires high electron density. Hence the calculated signal at 154.8 ppm with its experimental counterpart near 149.5 ppm is assigned to C1 (Fig. 2). Similarly, the theoretical signal at δ_c 136.5 ppm with its experimental counterpart near 128 ppm was ascribed to the C4 due to the strong electronegative nature of the Cl11 (chlorine11) atom. C2 and C6 are located in the *meta* position to the oxygen atom, where the induction effect is strong. Further, the lone pair electrons on Cl9 and Cl13 conjugate with ring π charge. As a result, the calculated peaks at δ_c 130.3 and 132.3 ppm, with their experimental counterparts around δ_c 121 and 124.5 ppm, are attributed to C2 and C6, respectively. The relatively high calculated chemical shifts near δ_c 142.5 and 144.8 ppm, with their experimental counterparts around δ 132 and 134.5 ppm, are ascribed to C3 and C5, respectively. It should be noted that these signals were influenced by the lone pair electrons on Cl10 and Cl12, which conjugated with the ring π-charge. The calculated and experimental data were subjected to correlation analysis so as to quantify the disagreement between them (Fig. 3).

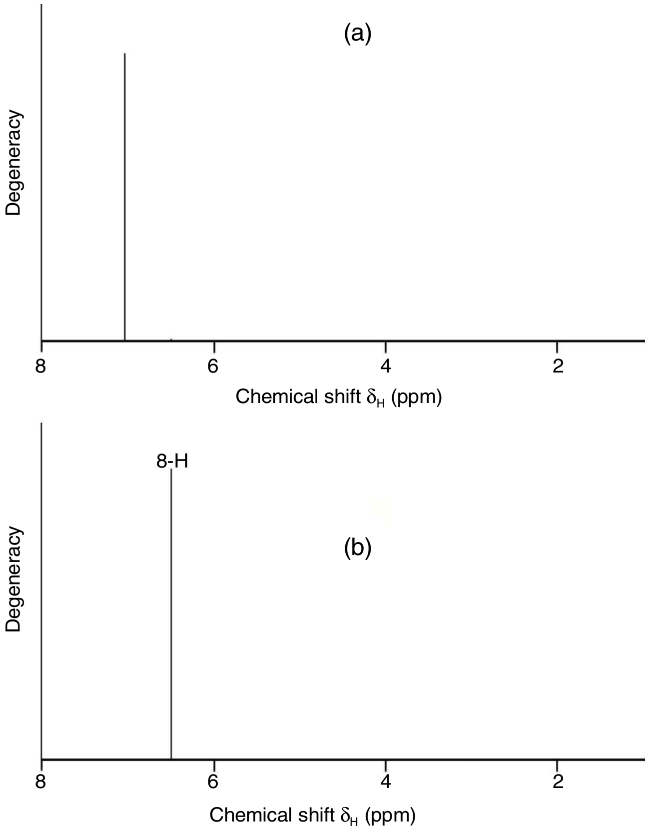

Fig. 1. ^{1}H NMR spectrum of pentachlorophenol (a) experimental and (b) simulated with FT/B3LYP/6-311++G(d,p) formalism

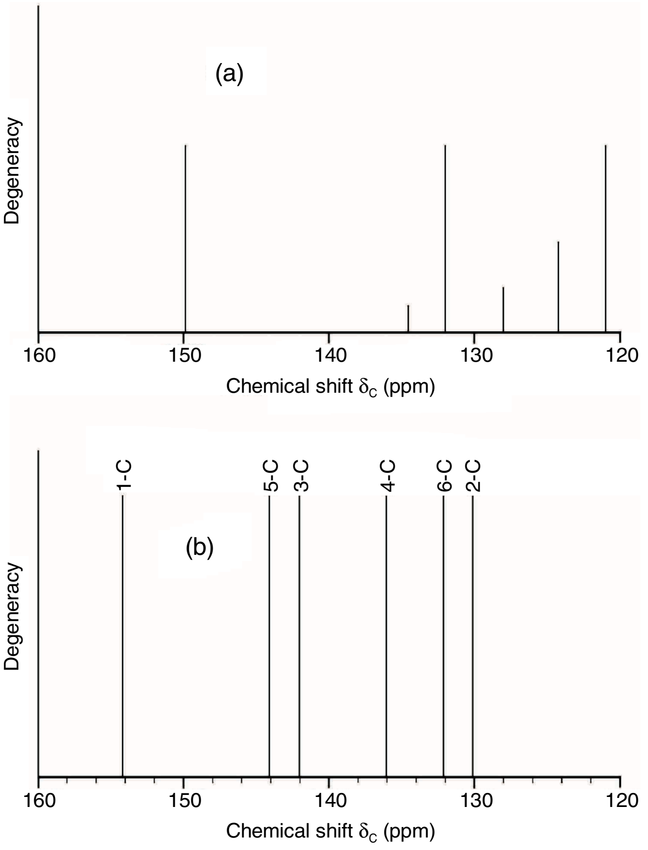

Fig. 2. ^{13}C NMR spectrum of pentachlorophenol (a) experimental and (b) simulated with DFT/B3LYP/6-311++G(d,p) formalism

TABLE-1
EXPERIMENTAL AND THEORETICAL CHEMICAL SHIFTS δ (ppm) OF PENTACHLOROPHENOL*

Atom	Experimental	Calculated
H(8)	7.2	6.6
C(1)	149.5	154.8
C(2)	121.0	130.3
C(3)	132.0	142.5
C(4)	128.0	136.5
C(5)	134.5	144.8
C(6)	124.5	132.3

*For numbering of atoms in pentachlorophenol, kindly refer the details in [Ref. 11]

The correlation coefficient obtained by DFT/B3LYP/6-311++ G(d,p) method for δ_C is $r^2 = 0.961$ for pentachlorophenol. This is fairly good and expected to reproduce the experimental data with fair amount of accuracy.

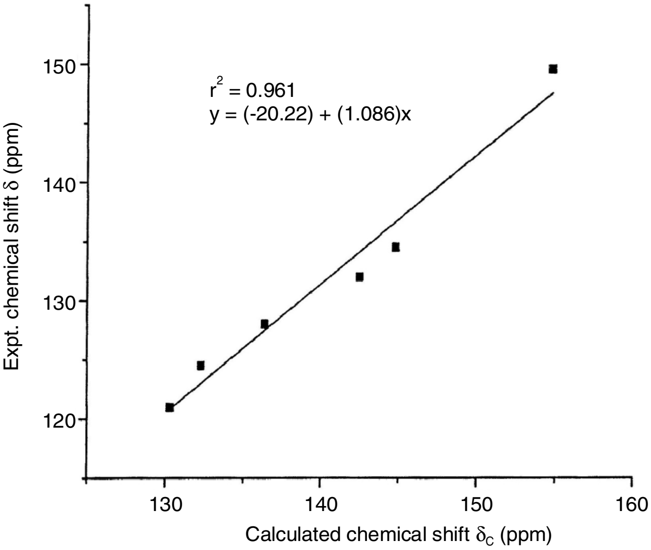

Fig. 3. Linear regression between the experimental and theoretical ^{13}C NMR chemical shifts of pentachlorophenol

Non-linear optical (NLO) properties: When electromagnetic radiation passes through NLO material, it interacts with the material. This interaction results in a change of phase, frequency, amplitude or other propagation characteristics of the incident radiation giving rise to new fields [30]. If these changes are significant then the NLO material may be used for optical logic, optical switching, optical memory and frequency shifting [31]. NLO effects of a given material are decided by the value of its first order hyperpolarizabilty. It is an accepted practice to determine the NLO behaviour of a given molecular system by comparing its total molecular dipole moment (μ_t) and mean first order hyperpolarizability (β_t) with corresponding value of urea. For urea, μ_t = 1.3732 Debye and β_t = 372.8 × 10^{-33} cm^5/e.s.u. For the molecule under investigation, the calculated values of μ_t and β_t were 0.6907 Debye and 51.7867 × 10^{-33} cm^5/e.s.u, respectively (Table-2). The values of μ_t and β_t of pentachlorophenol are very low in comparison with the corresponding values of urea. Hence, it can be concluded that pentachlorophenol is not useful as NLO material.

TABLE-2
VALUES OF DIPOLE MOMENT, μ_t (Debye); POLARIZABILITY, α_t (1.4818×10^{-25} cm^3); AND FIRST ORDER HYPERPOLARIZABILITY, β_t (8.641×10^{-33} cm^5/e.s.u) of PENTACHLOROPHENOL

Type of component	Value with B3LYP/6-311++G(d,p)	Type of component	Value with B3LYP/6-311++G(d,p)
μ_x	-0.5488	β_{xxx}	7.2756
μ_y	-0.4193	β_{xxy}	0.2435
μ_z	-0.0000	β_{xyy}	2.3469
μ_t	0.6907	β_{yyy}	35.2573
α_{xx}	178.0086	β_{xxz}	-0.0017
α_{xy}	-0.3557	β_{xyz}	-0.0010
α_{yy}	164.5693	β_{yyz}	-0.0009
α_{xz}	-0.0000	β_{xzz}	16.3353
α_{yz}	-0.0000	β_{yzz}	9.3103
α_{zz}	71.2018	β_{zzz}	-0.0002
α_t	137.9266	β_t	51.7867
$\Delta\alpha$	100.7609		

Frontier molecular orbitals (FMO): Important HOMO and LUMO molecular orbitals involved in electronic transition in pentachlorophenol are shown in Fig. 4. This can conveniently be used to explain the UV-visible spectra of molecules and chemical reactivity of conjugated systems.

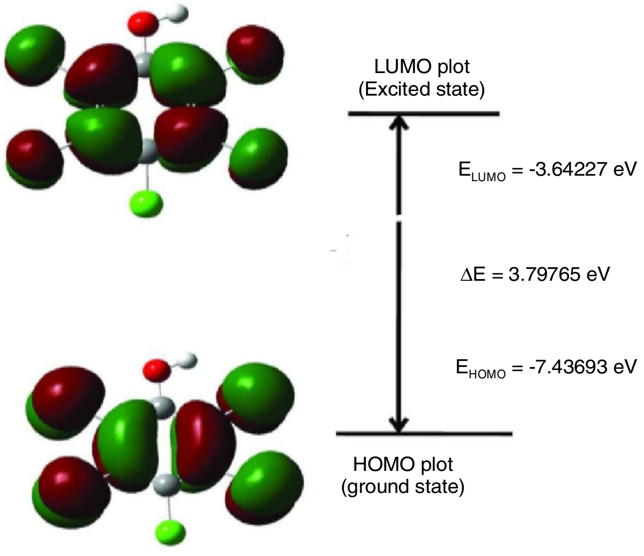

Fig. 4. Frontier molecular orbitals of pentachlorophenol

UV-visible spectrum: Experimental UV-visible absorption band arising due to electronic transition is shown in Fig. 5a for pentachlorophenol. It is compared with its simulated counterpart generated by TD-DFT/B3LYP/6-311++G(d,p) in Fig. 5b. According to calculations, pentachlorophenol should have one electronic transition at λ_{max} = 273.4 nm, with corresponding oscillator strength (*f*) = 0.0406. This agrees excellently with corresponding observed electronic transition at λ_{max} = 273 nm. Frontier molecular orbital study shows that the above experimental band arises due to H→L transition (H and L denote HOMO and LUMO, respectively). On analyzing molecular orbital coefficients, it is found that H→L electronic transition corresponds to n→π* excitation.

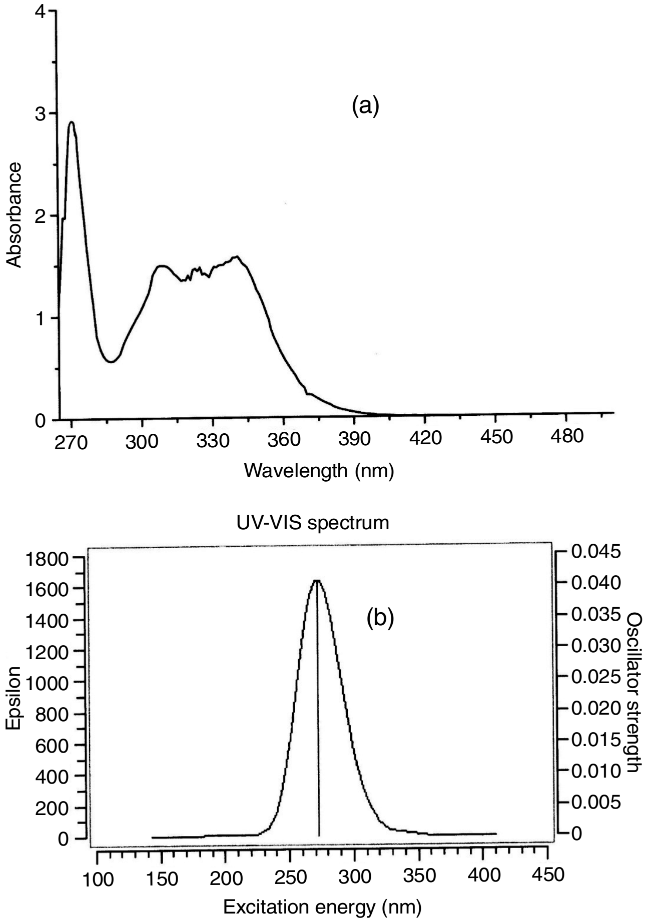

Fig. 5. UV-Vis spectrum of pentachlorophenol: (a) experimental and (b) simulated with DFT/B3LYP/6311++G(d,p) formalism

Chemical reactivity: Frontier molecular orbital parameters computed for pentachlorophenol, using DFT/B3LYP/6-311++G(d,p) are shown in Table-3. The difference between the HOMO and LUMO orbital energy is known as the energy gap and estimated at 3.7976 eV, for the molecule under consideration, in gaseous phase. This is a comparatively low value, characteristic of conjugated systems (Table-3). This implies that pentachlorophenol has high chemical reactivity, as it is energetically favourable to accumulate electrons in high lying LUMO by exciting electrons from low-lying HOMO. Further, as the chemical potential (μ) for pentachlorophenol is negative, it should be stable [32].

TABLE-3
FRONTIER MOLECULAR ORBITAL PARAMETERS OF PENTACHLOROPHENOL BY DFT/B3LYP/6-311++G(d,p) METHOD

Frontier molecular orbital parmeter	Value (eV)
HOMO energy	-7.4369
LUMO energy	-3.6422
Frontier molecular orbital energy gap	3.7976
Ionization energy (I)	7.4369
Electron affinity (A)	3.6422
Global chemical hardness (η)	1.8973
Global chemical softness (S)	0.2635
Chemical potential (μ)	-5.5395
Global electrophilicity index (ω)	8.0866

TABLE-4
SECOND-ORDER PERTURBATION THEORY ANALYSIS OF FOCK MATRIX IN NBO BASIS CORRESPONDING TO THE INTRA-MOLECULAR BONDS OF PENTACHLOROPHENOL BY DFT/B3LYP/6-311++G(d,p) METHOD (ONLY MAJOR CONTRIBUTORS TO STABILIZATION ENERGY ARE GIVEN)

Donor NBO(i)	Type of bond	Occupancy	Acceptor NBO(j)	Type of bond	Occupancy	$E(2)^a$ (kcal/mol)	$E(j)-E(i)^b$ (a.u)	$F(i,j)^c$ (a.u)
C1-C2	π	1.67377	C3-C4	π*	0.47951	22.39	0.28	0.073
			C5-C6	π*	0.47281	15.63	0.28	0.061
C3-C4	π	1.71140	C1-C2	π*	0.45440	15.26	0.29	0.062
			C5-C6	π*	0.47281	19.414	0.28	0.069
C5-C6	π	1.71908	C1-C2	π*	0.45440	20.40	0.29	0.071
			C3-C4	π*	0.47951	16.33	0.28	0.063
LP(2)O7		1.85339	C1-C2	σ*	0.04112	33.91	0.32	0.102
LP(3)Cl9		1.93045	C1-C2	π*	0.45440	11.44	0.32	0.060
LP(3)Cl10		1.91199	C3-C4	π*	0.47951	15.32	0.30	0.068
LP(3)Cl11		1.91837	C3-C4	π*	0.47951	14.48	0.30	0.065
LP(3)Cl12		1.90975	C5-C6	π*	0.47281	15.56	0.30	0.068
LP(3)Cl13		1.91463	C5-C6	π*	0.47281	14.79	0.30	0.066

Molecular electrostatic potential (MESP) surface: The MESP plot is shown in Fig. 6. It reveals variations in charge distribution between different parts of the molecule. Following usual practice colour code is used to indicate such differences. Red is employed to show relatively negative region and green is used to mark relatively positive region. In pentachlorophenol, negative regions occur mainly over Cl and O atomic sites, attributable to the presence of lone pair electrons in them. The positive region is confined to the hydrogen atom.

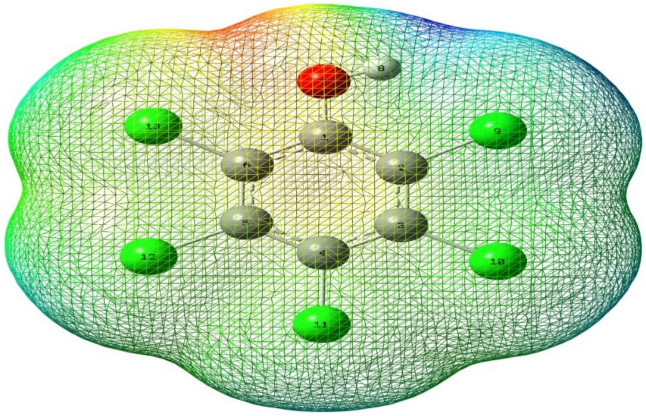

Fig. 6. Total electron density mapped with molecular electrostatic potential surface

Natural bond orbital (NBO) analysis: The NBO analysis enables us to understand delocalization effects such as intra- and intermolecular bonding, interaction among bonds and interactions involving bonding and antibonding orbitals, in terms of intramolecular charge transfer (ICT) from the highest occupied bonding orbitals to unoccupied antibonding orbitals of a molecular system. In pentachlorophenol, the ICT is a result of overlapping of σ(C-C) and π(C-C) bonding orbitals with their corresponding antibonding orbitals σ*(C-C) and π*(C-C), respectively. Consequently, the electron density in the (C-C) antibonding orbitals increases, leading to weakening of the respective bonds. The electron density at six conjugative π-bonds (1.67-1.72e) and π*-bonds (0.45-0.48e) of the aromatic ring demonstrates strong delocalization contributing a total of 109.42 kcal mol^{-1} towards stabilization energy (Table-4). In addition, the lone pairs (LP) on oxygen and chlorine atoms also stabilize the system further. The contributions to stabilization energy from LP(2) O7, LP(3) Cl9, LP(3) Cl10, LP(3) Cl11, LP(3) Cl12 and LP(3) Cl13 by way of conjugative interaction (delocalization) through the bonds σ*(C1-C2), π*(C1-C2), π*(C3-C4), π*(C3-C4), π*(C5-C6) and π*(C5-C6) ranges from 33.91 to 11.44 kcal mol^{-1} (Table-4).

Thermodynamic parameters: The standard thermodynamic functions, namely, heat capacity at constant pressure (C_P), heat capacity at constant volume (C_v) and entropy (S) were estimated on the basis of vibrational analysis and statistical thermodynamics, whereas other parameters, such as rotational constants (A, B, C), zero point vibrational energy (E_o) and self-consistent field (SCF) energy were computed for pentachlorophenol by DFT method with B3LYP/6-311++G(d,p) and were depicted in Table-5.

TABLE-5
THERMODYNAMIC PARAMETERS (FOR ONE MOLE OF PERFECT GAS AT ONE ATM.) AND ROTATIONAL CONSTANTS OF PENTACHLOROPHENOL

Thermodynamic parameters	Values
SCF energy (Hartree)	-2605.6424
Total energy (thermal), E_{total} (kcal mol^{-1})	42.6260
Heat capacity at const. volume, C_v (cal mol^{-1} K^{-1})	40.7170
Heat capacity at const. presure, C_p (cal mol^{-1} K^{-1})	42.7028
Entropy, S (cal mol^{-1} K^{-1})	108.655
Vibrational energy, E_{vib} (kcal mol^{-1})	40.8490
Zero-point vibrational energy, E_0 (kcal mol^{-1})	-35.3524
Rotational constants (GHz)	
A	0.5704
B	0.4620
C	0.2552

Conclusion

The density functional theory at DFT-B3LYP/6-31+G (d,p) level is compatible for geometry optimization without introducing the conformational changes evident from the fair agreement between theoretical and experimental spectral characteristics (IR [11], NMR and UV-visible) of pentachlorophenol. The results indicated that there was a close agreement between the observed and corresponding predicted proton NMR chemical shifts of pentachlorophenol. The same was also true of its ^{13}C NMR signals. There was a close agreement between the measured UV-visible spectrum of pentachlorophenol, with its computed counterpart. Electronic parameters such as HOMO-LUMO energies, their energy gap, ionization potential, electron affinity were also computed from DFT studies. Moreover, the studied molecule was not a NLO material. The NBO analysis identified the localized bonding and anti-bonding orbitals, which stabilized pentachlorophenol through delocalization and intramolecular charge transfer.

ACKNOWLEDGEMENTS

The authors are thankful to National Institute of Technology, Warangal, India, for providing spectral measurements. First two authors are grateful to the management of SR University, Warangal, India, for facilitating this research work.

CONFLICT OF INTEREST

The authors declare that there is no conflict of interests regarding the publication of this article.

REFERENCES

1. A.T. Proudfoot, *Toxicol. Rev*., **22**, 3 (2003); https://doi.org/10.2165/00139709-200322010-00002
2. B.G. Reigner, R.A. Gungon, F.Y. Bois, L. Zeise and T.N. Tozer, *J. Pharm. Sci*., **81**, 1113 (1992); https://doi.org/10.1002/jps.2600811115
3. M.S. Salkinoja-Salonen, P.J.M. Middeldorp, M. Briglia, R.J. Valo, M.M. Haggblom. A. McBain and J.H.A. Apajalahti. *Adv. Appl. Biotechnol*., **4**, 347 (1989).
4. M.M. Laine and K.S. Jørgensen, *Appl. Environ. Microbiol.*, **62**, 1507 (1996); https://doi.org/10.1128/aem.62.5.1507-1513.1996
5. C.S. Orser and C.C. Lange, *Biodegradation*, **5**, 277 (1994); https://doi.org/10.1007/BF00696465
6. M. Czaplicka, *Sci. Total Environ*., **322**, 21 (2004); https://doi.org/10.1016/j.scitotenv.2003.09.015
7. P.V. Ramana Rao and G.R. Rao, *Spectrochim. Acta A Mol. Biomol. Spectrosc.*, **58**, 3039 (2002); https://doi.org/10.1016/S1386-1425(02)00101-4
8. P.V. Ramana Rao and G.R. Rao, *Spectrochim. Acta A Mol. Biomol. Spectrosc.*, **58**, 3205 (2002); https://doi.org/10.1016/S1386-1425(02)00102-6
9. K. Srishailam, B.V. Reddy and G.R. Rao, *J. Mol. Struct.*, **1196**, 139 (2019); https://doi.org/10.1016/j.molstruc.2019.06.064
10. K. Ramaiah, K. Srishailam, K.L. Reddy, B.V. Reddy and G.R. Rao, *J. Mol. Struct.*, **1184**, 405 (2019); https://doi.org/10.1016/j.molstruc.2019.02.060
11. K. Srishailam, P.V. Ramana Rao, L. Ravindranath, B.V. Reddy and G.R. Rao, *J. Mol. Struct.*, **1178**, 142 (2019); https://doi.org/10.1016/j.molstruc.2018.10.022
12. P.V. Ramana Rao, K. Srishailam, L. Ravindranath, B.V. Reddy and G.R. Rao, *J. Mol. Struct.*, **1180**, 665 (2019); https://doi.org/10.1016/j.molstruc.2018.12.036
13. M.J. Frisch, G.W. Trucks, H.B. Schlegel, G.E. Scuseria, M.A. Robb, J.R. Cheeseman, G. Scalmani, V. Barone, B. Mennucci, G.A. Petersson, H. Nakatsuji, M. Caricato, X. Li, H.P. Hratchian, A.F. Izmaylov, J. Bloino, G. Zheng, J.L. Sonnenberg, M. Hada, M. Ehara, K. Toyota, R. Fukuda, J. Hasegawa, M. Ishida, T. Nakajima, Y. Honda, O. Kitao, H. Nakai, T. Vreven, J.A. Montgomery, Jr., J.E. Peralta, F. Ogliaro, M. Bearpark, J.J. Heyd, E. Brothers, K.N. Kudin, V.N. Staroverov, T. Keith, R. Kobayashi, J. Normand, K. Raghavachari, A. Rendell, J.C. Burant, S.S. Iyengar, J. Tomasi, M. Cossi, N. Rega, J.M. Millam, M. Klene, J.E. Knox, J.B. Cross, V. Bakken, C. Adamo, J. Jaramillo, R. Gomperts, R.E. Stratmann, O. Yazyev, A.J. Austin, R. Cammi, C. Pomelli, J.W. Ochterski, R.L. Martin, K. Morokuma, V.G. Zakrzewski, G.A. Voth, P. Salvador, J.J. Dannenberg, S. Dapprich, A.D. Daniels, O. Farkas, J.B. Foresman, J.V. Ortiz, J. Cioslowski and D.J. Fox, Gaussian 09, Revision B.01; Gaussian, Inc., Wallingford CT (2010).
14. A.D. Becke, *J. Chem. Phys.*, **98**, 5648 (1993); https://doi.org/10.1063/1.464913
15. C. Lee, W.T. Yang and R.G. Parr, *Phys. Rev. B Condens. Matter*, **37**, 785 (1988); https://doi.org/10.1103/PhysRevB.37.785
16. K. Wolinski, R. Haacke, J.F. Hinton and P. Pulay, *J. Comput. Chem.*, **18**, 816 (1997); https://doi.org/10.1002/(SICI)1096-987X(19970430)18:6<816::AID-JCC7>3.0.CO;2-V
17. G. Scalmani and M.J. Frisch, *J. Chem. Phys.*, **132**, 114110 (2010); https://doi.org/10.1063/1.3359469
18. R. Improta, V. Barone, G. Scalmani and M.J. Frisch, *J. Chem. Phys.*, **125**, 054103 (2006); https://doi.org/10.1063/1.2222364
19. R. Improta, G. Scalmani, M.J. Frisch and V. Barone, *J. Chem. Phys.*, **127**, 074504 (2007); https://doi.org/10.1063/1.2757168
20. A.D. Buckingham, eds.: Joseph O. Hirschfelder, Permanent and Induced Molecular Moments and Long-Range Intermolecular Forces, In Advances in Chemical Physics: Intermolecular Forces, John Wiley & Sons, Inc., volume 12, p. 107 (1967).
21. D.A. McQuarrie, Thermodynamics, Harper and Row: New York (1973).
22. G. Gece, *Corros. Sci.*, **50**, 2981 (2008); https://doi.org/10.1016/j.corsci.2008.08.043
23. K. Fukui, *Science*, **218**, 747 (1982); https://doi.org/10.1126/science.218.4574.747
24. T. Koopmans, *Physica*, **1**, 104 (1933); https://doi.org/10.1016/S0031-8914(34)90011-2
25. R.G. Parr, L.V. Szentpa'ly and S. Liu, *J. Am. Chem. Soc.*, **121**, 1922 (1999); https://doi.org/10.1021/ja983494x
26. N. Özdemir, B. Eren, M. Dincer and Y. Bekdemir, *Mol. Phys.*, **108**, 13 (2010); https://doi.org/10.1080/00268970903476688
27. P. Politzer and J.S. Murray, *Theor. Chem. Acc.*, **108**, 134 (2002); https://doi.org/10.1007/s00214-002-0363-9
28. A.E. Reed, L.A. Curtiss and F. Weinhold, *Chem. Rev.*, **88**, 899 (1988); https://doi.org/10.1021/cr00088a005
29. J. Chocholoušová, V. Špirko and P. Hobza, *Phys. Chem. Chem. Phys.*, **6**, 37 (2004); https://doi.org/10.1039/B314148A
30. C. Andraud, T. Brotin, C. Garcia, F. Pelle, P. Goldner, B. Bigot and A. Collet, *J. Am. Chem. Soc.*, **116**, 2094 (1994); https://doi.org/10.1021/ja00084a055
31. V.M. Geskin, C. Lambert and J.L. Bredas, *J. Am. Chem. Soc.*, **125**, 15651 (2003); https://doi.org/10.1021/ja035862p
32. M. Nakano, H. Fujita, M. Takahata and K. Yamaguchi, *J. Am. Chem. Soc.*, **124**, 9648 (2002); https://doi.org/10.1021/ja0115969